10-2018

Thermal environment sensor array: Part 1 development and field performance assessment

Brett C. Ramirez
Iowa State University, bramirez@iastate.edu

Yun Gao
Iowa State University and Huazhong Agricultural University

Steven J. Hoff
Iowa State University

Jay D. Harmon
Iowa State University, jharmon@iastate.edu

Thermal environment sensor array: Part 1 development and field performance assessment

Abstract
Current thermal environment (TE) monitoring and control strategies for livestock and poultry facilities require enhanced measurement capabilities to provide an optimum TE based on the animals' thermal demands. Further, techniques for combining additional parameters are needed to adequately assess the total impact of the TE on the animals. Hence, two papers introduce a spatial network of 44 Thermal Environment Sensor Arrays (TESAs), each with a custom data acquisition system (Part 1) and a technique for evaluating the TE as a function of mean body temperature difference from thermally comfortable pigs using estimated body mass and TESA measurements as inputs (Part 2). The TESAs and new thermal index were deployed in a commercial pig facility to perform a preliminary assessment of robustness and capabilities under production settings. Each TESA measured dry-bulb temperature (Tdb), black globe temperature, airspeed, and relative humidity (RH), and required a custom circuit board with a microcontroller, signal conditioning, and communication hardware. After closeout (completion of the production cycle), TESAs were validated with a reference system to determine individual time constants and assess if a significant bias correction was needed (except airspeed). Total number of usable measurements for subsequent analysis for all sensors per TESA averaged (95% CI) 202,310 (199,187; 205,437). In summary, 7% Tdb thermistor, 9% digital Tdb, and 27% RH sensors required correction after 170 d inside the facility. Utilisation of low-cost sensors, open-source software, and microcontrollers allowed this novel network to provide sufficient measurement density to promote future queries on TE data in animal facilities.

Keywords
Pigs, Data acquisition, Microcontroller, Ventilation, Precision livestock farming

Disciplines
Agriculture | Bioresource and Agricultural Engineering | Other Animal Sciences

Comments
This is a manuscript of an article published as Ramirez, Brett C., Yun Gao, Steven J. Hoff, and Jay D. Harmon. "Thermal environment sensor array: Part 1 development and field performance assessment." *Biosystems Engineering* 174 (2018): 329-340. DOI: 10.1016/j.biosystemseng.2018.08.002. Posted with permission.

Thermal environment sensor array: Part 1 Development and field performance assessment

Brett C. Ramirez[1], Yun Gao[1,2], Steven J. Hoff[1], and Jay D. Harmon[1]

[1] Department of Agricultural and Biosystems Engineering, Iowa State University, Ames, IA, USA

[2] College of Engineering, Huazhong Agricultural University and the Cooperative Innovation Center for Sustainable Pig Production, Wuhan, China

Corresponding author: Brett C. Ramirez, Department of Agricultural and Biosystems Engineering, Iowa State University, 605 Bissell Road; 4348 Elings Hall, Ames, IA, 50011, USA; phone: (515) 294 0468; e-mail: bramirez@iastate.edu.

Abstract. Current thermal environment (TE) monitoring and control strategies for livestock and poultry facilities require enhanced measurement capabilities to provide an optimum TE based on the animals' thermal demands. Further, techniques for combining additional parameters are needed to adequately assess the total impact of the TE on the animals. Hence, two papers introduce a spatial network of 44 Thermal Environment Sensor Arrays (TESAs), each with a custom data acquisition system (Part 1) and a technique for evaluating the TE as a function of mean body temperature difference from thermally comfortable pigs using estimated body mass and TESA measurements as inputs (Part 2). The TESAs and new thermal index were deployed in a commercial pig facility to perform a preliminary assessment of robustness and capabilities under production settings. Each TESA measured dry-bulb temperature (T_{db}), black globe temperature, airspeed, and relative humidity (RH), and required a custom circuit board with a microcontroller, signal conditioning, and communication hardware. After closeout (completion of the production cycle), TESAs were validated with a reference system to determine individual time constants and assess if a significant bias correction was needed (except airspeed). Total number of usable measurements for subsequent analysis for all sensors per TESA averaged (95% CI) 202,310 (199,187; 205,437). In summary, 7% T_{db} thermistor, 9% digital T_{db}, and 27% RH

sensors required correction after 170 d inside the facility. Utilisation of low-cost sensors, open-source software, and microcontrollers allowed this novel network to provide sufficient measurement density to promote future queries on TE data in animal facilities.

Keywords. pigs; data acquisition; microcontroller; ventilation; precision livestock farming

Nomenclature.

ADC	Analogue to Digital Converter
BGT	Black Globe Thermometer
CDMS	Custom Data Management Software
CI	Confidence Interval
CTA	Constant Temperature Anemometer
DAQ	Data Acquisition
MTRHR	Mobile Temperature and Relative Humidity Reference
n	number of steady-state measurements
NTC	Negative Temperature Coefficient
OTA	Omnidirectional Thermal Anemometer
PCB	Printed Circuit Board
RH	Relative Humidity (%)
s_{ref}	steady-state standard deviation for reference sensor (°C or % RH)
s_{TESA}	steady-state standard deviation for TESA sensor (°C or % RH)
t	time (s)
t_0	initial time (s)
τ	time constant (s)
T_{db}	dry-bulb temperature (°C)
TE	Thermal Environment
TESA	Thermal Environment Sensor Array
TESA DAQ	Thermal Environment Sensor Array Data Acquisition
T_g	globe temperature (°C)
T_{mr}	mean radiant temperature (°C)
$x(t)$	sensor response as a function of time (°C or % RH)
x_0	initial mean sensor value at time t_0 (°C or % RH)
$\bar{x}_{ref}$	mean reference steady-state value (°C or % RH)
x'^*_{TESA}	bias corrected future measure value (°C or % RH)
x'_{TESA}	future measured value (°C or % RH)
z_{calc}	z-statistic
ΔR_{ref}	divider resistor standard uncertainty (reference; Ω)
$\Delta^0 RH$	relative humidity zeroth-order standard uncertainty
$\Delta^0 RH_{ref}$	reference RH zeroth-order standard uncertainty
$\Delta^0 T_{db}$	dry-bulb temperature zeroth-order standard uncertainty (analogue)
$\Delta^0 T_{db,d}$	dry-bulb temperature zeroth-order standard uncertainty (digital)
$\Delta^0 T_g$	globe temperature zeroth-order standard uncertainty

$\Delta^0 T_{ref}$	reference T_{db} zeroth-order standard uncertainty
$\Delta^0 u$	airspeed zeroth-order standard uncertainty
ΔV_{ref}	analogue voltage standard uncertainty (reference; V_{DC})
Δx	difference between x_0 and x at steady-state (°C or % RH)
Δx_{ref}	single sample reference standard uncertainty (°C or % RH)
$\Delta \bar{x}_{ref}$	mean steady-state reference combined standard uncertainty (°C or % RH)
$\Delta^0 x_{ref}$	zeroth-order standard uncertainty for reference sensor (°C or % RH)
$\Delta \bar{x}_{TESA}$	mean steady-state TESA combined standard uncertainty (°C or % RH)
$\Delta^0 x_{TESA}$	zeroth-order standard uncertainty for TESA sensor (°C or % RH)
$\Delta \bar{x}_{TESA}$	mean TESA sensor steady-state value (°C or % RH)

1 Introduction

The growing global population is projected to increase by 2.4 billion people from 2015 to 2050 (UN, 2015) and will require a secure animal-based protein supply raised in energy, water, and feed efficient housing systems that do not adversely impact the environment. A housing system operating within the animal's optimum Thermal Environment (TE) is one approach to enhance animal well-being and growth performance (Curtis, 1983; Renaudeau, Gourdine, & St-Pierre, 2011), while simultaneously reducing facility resource usage, as well as total feed consumed and days on feed. The TE describes the parameters that influence heat exchange (i.e., convective, conductive, radiative, and evaporative) between an animal and its surroundings (ASHRAE, 2013; Curtis, 1983; DeShazer, Hahn, & Xin, 2009); however, all required parameters that describe the TE a housed animal experiences are rarely quantified, resulting in a lack of accurate TE control that is optimal for the animal. Hence, there is a need for advanced techniques to accurately assess and, ultimately, control the TE based on how the animal exchanges heat with its surroundings (Fournel, Rousseau, & Laberge, 2017).

The parameters used to describe the TE include dry-bulb temperature (T_{db}), relative humidity (RH), airspeed, and mean radiant temperature (T_{mr}). Dry-bulb temperature is frequently the main parameter used to describe and control TE in commercial animal production systems; however, it exclusively impacts the convective (with airspeed) and evaporative (with airspeed and RH) modes of heat loss. The RH must be known with T_{db} to estimate latent heat loss (i.e., by respiration or wetted skin evaporation) by determining the water vapour pressure gradient between surrounding air and the saturated surface. Airspeed influences convective and evaporative heat transfer rates, and can substantially increase heat loss (beneficial in a hot T_{db}; unfavourable in a cold T_{db}). Lastly, T_{mr} is the uniform temperature of the surroundings in which radiant heat transfer from the animal's surface equals that in the actual surroundings. Due to the instrumentation difficulties, T_{mr} and airspeed are often neglected in livestock facilities, despite Bond et al. (1952), Mount (1967), Mount (1964), and Beckett (1965) having shown radiative

heat losses to be a substantial source of heat loss from pigs.

The incorporation of these four parameters into a single Thermal Environment Sensor Array (TESA) that is robust and practical for application in livestock and poultry facilities would allow the integration and application of advanced techniques. For human occupied buildings, many commercially available TE measurement systems exist to quantify indoor thermal comfort statistical values (e.g., draught rate, predicted mean vote, and predicted percentage dissatisfied; ASHRAE, 2013). These systems are prohibited by cost from use in multi-point Data Acquisition (DAQ) systems, feature proprietary hardware and software that limit flexibility, and are designed for relatively clean, low airspeed environments. In animal production systems, various combinations of T_{db}, RH, airspeed, and/or T_{mr} have been monitored (Brown-Brandl et al., 2014; Hayes et al., 2013; Vilela et al., 2015), but rarely all together. There is a unique opportunity, specific to animal production systems, for a sensor network that focuses on the TE demands of the animal.

In this study, a TESA and DAQ were developed and validated with a well-documented statement of measurement uncertainty for capturing the TE spatial and temporal distribution in pig facilities. This system was developed to simultaneously quantify the TE the animals experience in order to enable an animal-centric approach to pig production. The utilisation of low-cost sensors, open-source software, and microcontroller-based control allows this novel network of TESAs and accompanying DAQ to provide sufficient measurement density that design and control of TE modification systems can be adjusted to enhance and maintain the optimal TE for improved animal production efficiency and thermal comfort. Hence, the objectives of this research were: (1) develop TESA and accompanying DAQ; (2) deploy 44 TESAs in a deep-pit, wean-finish pig barn for six months to assess system robustness and accuracy over time; and (3) make a preliminary assessment of the TE under normal production operating conditions.

2 Materials and methods

2.1 Thermal environment sensor array

An individual Thermal Environment Sensor Array (TESA; Figure 1) was developed to measure dry-bulb temperature (T_{db}), relative humidity (RH), airspeed, and estimate mean radiant temperature (T_{mr}) from the globe temperature (T_g) of a Black Globe Thermometer (BGT). Sensor signals from a TESA were connected via a 3.05 m long, nine-conductor wire to screw terminals mounted on the TESA Data Acquisition (TESA DAQ) custom Printed Circuit Board (PCB).

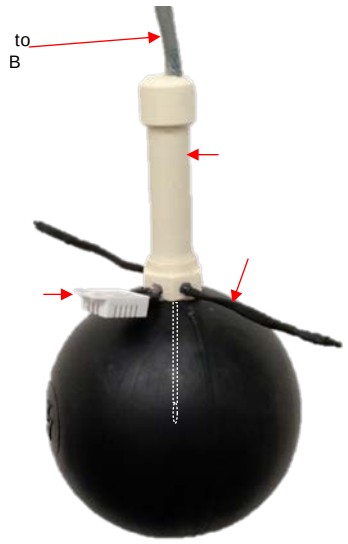

Figure 1. A Thermal Environment Sensor Array (TESA) featuring dry-bulb temperature, relative humidity, airspeed, and black globe thermometer sensors. Globe temperature is obtained from a dry-bulb temperature sensor secured at the centre of the black globe thermometer.

2.1.1 Sensors

Ambient T_{db} and T_g were measured with a Negative Temperature Coefficient (NTC) thermistor (nominal 10 kΩ at 25 °C, NTCLE413E2103F, Vishay, Malvern, PA, USA; Figure 1). Gao, Ramirez, & Hoff (2016) provide further details regarding the signal conditioning and nonlinear regression coefficients for these two thermistors. Additionally, a single wire, digital interface $T_{db,d}$ and RH sensor (RHT03, MaxDetect Technology Co. Ltd., Shenzhen, China; Figure 1) was used. Valid sensor operation ranged from -40 °C to 80 °C ($T_{db,d}$) and 0% to 100%

(RH; non-condensing).

A custom Omnidirectional Thermal Anemometer (OTA; Figure 1) was developed to measure airspeeds between 0 and 5.5 m s^{-1}. A near-spherical, NTC thermistor (nominal 470 Ω at 25 °C, Model LC471F3K, U.S. Sensor Corp., Orange, CA, USA) was heated above ambient T_{db} by a Constant Temperature Anemometer (CTA) circuit in order to estimate the electrical power dissipated by the OTA as a function of airspeed and the fluid properties of the air for a given T_{db}. Gao et al. (2016) provide further detail regarding the sensor design, calibration, and T_{db} compensation approach.

The net exchange of radiant energy between objects is the algebraic sum of all the radiant fluxes in which the object is exposed. Dimensions, locations, and thermal characteristics (i.e., surface temperature and emissivity) of the surrounding exposed objects must be known to calculate the flux of each object; however, this method becomes increasingly difficult and time consuming to implement when the number of sources is large and geometries complex (ASHRAE, 2013; ISO 7726, 2001, p. 77). The BGT is a cost effective and simple approach to estimate T_{mr} when coupled with ambient T_{db} and airspeed measurements at the level of the BGT (Bond & Kelly, 1955; Pereira, Bond, & Morrison, 1967; Purswell & Davis, 2008). A BGT (Figure 1) was constructed from a 0.1016 m diameter, flat black, hollow plastic sphere (3FXE7, W.W. Grainger Inc.) with a nominal 1.27 cm CPVC male adapter threaded into a 0.635 cm diameter hole in the top of the plastic sphere. This size was chosen to reduce the size and mass of the TESA, and reduce swinging of TESA at high airspeeds. Outer emissivity was assumed to be 0.95 (ASHRAE, 2013) and the plastic sphere wall thickness was 0.81 mm. A rubber stopper with a small axial hole was inserted into the CPVC male adapter to secure the T_{db} thermistor at the centre of the BGT.

2.1.2 Zeroth-order uncertainty analysis

A zeroth-order uncertainty budget, including Type A (the best available estimate of the expected value of a quantity that varies randomly) and Type B (not obtained from repeated

observation, rather based on all available information) evaluations, was created for each TESA sensor. Results from the zeroth-order uncertainty budget were then propagated through any analytical solutions that use measurements as inputs, to ultimately determine the combined standard uncertainty (denoted by Δ) associated with the calculated value.

The procedure to compute the combined standard uncertainty associated with the TESA DAQ microcontroller analogue to digital conversion, T_{db} and T_g measurement (via NTC thermistor), and airspeed measurement are reported in Gao et al. (2016). Contributors to the zeroth-order uncertainty for the digital T_{db} and RH sensor (provided by the manufacturer) were the stated accuracy (±0.5 °C; ±2% RH), reading resolution (±0.1 °C; ±0.1% RH), repeatability (±0.2 °C; ±1% RH), RH hysteresis (±0.3%), and RH long-term stability (±0.5%), and also assumed to have a rectangular probability distribution because no information is provided regarding the source of the values; hence, values are assumed to have an equal probability of existing within the stated range. The results of the zeroth-order uncertainty budget for all the sensors and computed value are summarised in Table 1.

Table 1. Zeroth-order uncertainty budget summary for TESA sensors.

Parameter	Description	Sensor	Interface	Zeroth-order standard uncertainty (Δ^0_x)		Unit
T_{db}	Dry-bulb temperature	NTC thermistor	Analogue	$\Delta^0 T_{db}$	= 0.33	°C
$T_{db,d}$	Dry-bulb temperature	AMig	Digital	$\Delta^0 T_{db,d}$	= 0.31	°C
RH	Relative humidity	Polymer humidity capacitor	Digital	$\Delta^0 RH$	= 1.33	% RH
u	Airspeed	OTA	Analog	$\Delta^0 u$	= 0.11 (at 0.47 m s^{-1}) to 0.71 (at 5.52 m s^{-1})	m s^{-1}
T_g	Globe temperature	NTC thermistor	Analog	$\Delta^0 T_g$	= 0.33	°C

2.2 Data acquisition and serial communication

The TESA DAQ featured a custom designed (Eagle v7.4, CadSoft Computer GmbH, Pleiskirchen, Germany) and manufactured PCB (OSH Park; https://oshpark.com/) for containing the signal conditioning circuits (Figure 2).

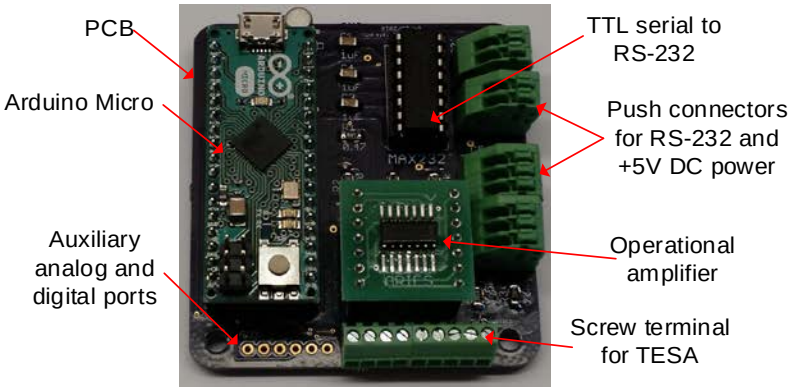

Figure 2. Thermal Environment Sensor Array Data Acquisition (TESA DAQ) on the custom Printed Circuit Board (PCB) with microcontroller, signal conditioning, and serial communication for a single TESA.

2.2.1 Printed circuit board and housing

The PCB (Figure 2) included the CTA circuit, T_{db} divider circuits, a microcontroller (Arduino Micro, Arduino LLC, Italy), and a serial TTL to RS-232 converter (MAX232IN, Texas Instruments Inc., Dallas, TX, USA). The operational amplifier in the CTA circuit was replaceable if the device failed or needed replacement. Similarly, the microcontroller could be readily removed for programming or replacement. Eight capacitors (each 1 µF) were required for the serial TTL to RS-232 converter, in addition to one 10 kΩ resistor for the digital T_{db} and RH sensor.

Two TESA DAQs (i.e., one per TESA), stacked on top of each other, were housed in a 0.136 × 0.136 × 0.09 m (length × width × depth) weatherproof housing (NBF-32010, Bud Industries Inc., Willoughby, OH, USA) for protection from the environment (Figure 3). Four cable grips were installed to provide watertight connections for the two TESA signal wires, serial communication, and +5 V_{DC} power transformer (WSU050-1500, Triad Magnetics, Perris, CA, USA).

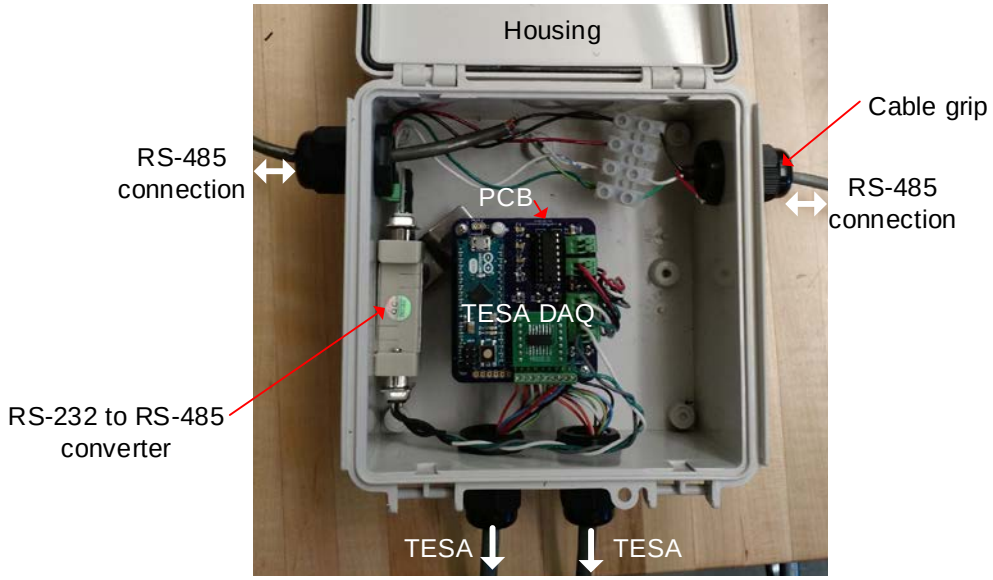

Figure 3. Weatherproof housing containing two TESA DAQ on PCBs (stacked) for deployment of two TESAs and serial communication hardware.

2.2.2 Serial communication network

The serial data communication network featured bidirectional data transfer between a notebook computer and every deployed TESA DAQ (Figure 4). A unique address identification number was programmed onto each TESA DAQ microcontroller such that a handshake protocol (bidirectional data transfer) could be implemented in a multipoint RS-485 network. On command, the terminal data communication device (i.e., TESA DAQ microcontroller) sent collected sensor data through a TTL serial to RS-232 converter (Figure 2) then a RS-232 to RS-485 converter (ATC-106, ATC Technology Co., Ltd, Wilmington, MA, USA; Figure 3). RS-485 was used due to its robustness and stability over long-distances in electrically noisy environments. A RS-485 bus to universal serial bus converter (USB-RS485-PCBA, FTDI Ltd, Glasgow, United Kingdom) was interfaced with the computer and a Custom Data Management Software (CDMS). TESA DAQs were arranged in series, that is, one three-conductor cable (+485, -485, ground) between each housing (one RS-232 to RS-485 converter per housing). This approach also minimised communication cable length and was relatively easy to implement, but with more labour than other communication protocols, such as wireless.

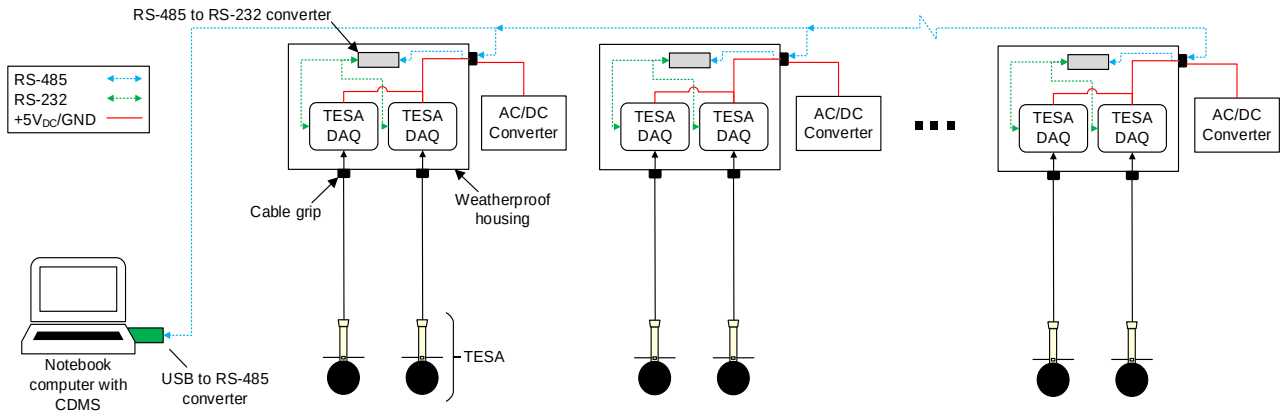

Figure 4. Schematic of serial communication network connecting two TESA DAQs per weatherproof housing together with the notebook.

2.2.3 Software

One TESA DAQ program (Figure 5a) was developed in the integrated development environment for the microcontroller and, when prompted by the CDMS (Python 2.7, Python Software Foundation, Beaverton, Oregon, USA; Figure 5b) on the computer, returned the mean of 20 sequentially measured (approximately every 2 ms) analogue voltages (two for airspeed, two for T_{db}), digital T_{db}/RH measurements, and time between analogue voltage measurements. The CDMS controlled sampling interval between data transmission requests to each TESA DAQ and timestamped incoming data.

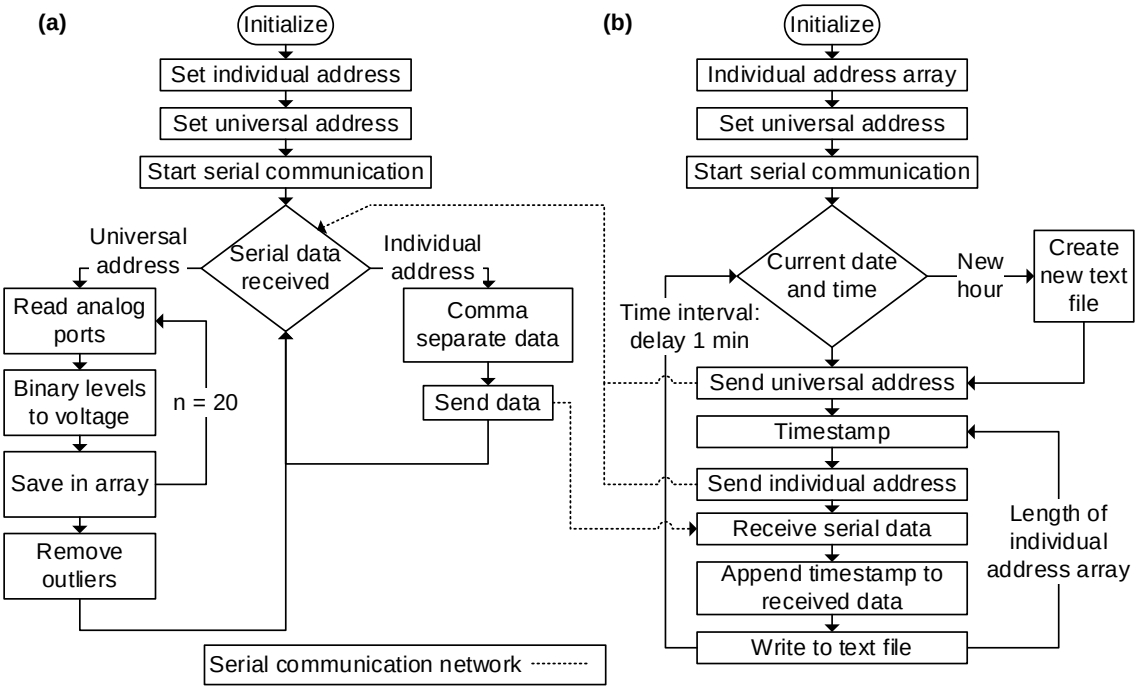

Figure 5. Pseudo algorithm for custom (a) TESA DAQ program (executed on microcontroller) and (b) CDMS software (executed on notebook computer). The universal address is a command for all TESAs to begin to measure values; while the individual address is to announce one TESA to send back data. The time interval between each loop in CDMS is adjustable to determine the sampling interval.

2.3 Field deployment

As part of a larger study, a total of 44 TESAs were deployed in a deep-pit, wean-finish pig facility located within 8.9 km of Pocahontas, IA, USA (42°44'04.2"N, 94°40'18.4"W) from August 8th, 2016 to January 25th, 2017 (Figure 6). The goal was to collect preliminary data on the ability of TESA to describe the TE inside each room under normal production operating conditions and then assess the robustness of TESA after a flow of pigs. The facility featured two side-by-side rooms, with room dimensions (length × width × height) of 61 m × 15.2 m × 2.54 m and each housing ~1200 pigs in 12 pens. The length of the building was orientated along the East-West axis. The negative pressure ventilation system was fully mechanical with power (i.e., fresh air distributed through ceiling inlets in cold to mild conditions) to tunnel (i.e., fresh air pulled the length of the building from the tunnel curtain at the one end wall to fans at the other end wall in hot conditions) operation. Ambient T_{db} and RH were recorded at the facility by the

ventilation controller every 15 min. A total of 22 TESAs were suspended about 1 m above the fully-slatted concrete floor in each room corresponding to Figure 6. A text file containing the comma-separated data from all 44 TESAs at a 1 min sampling interval was created and saved every hour on removable flash memory.

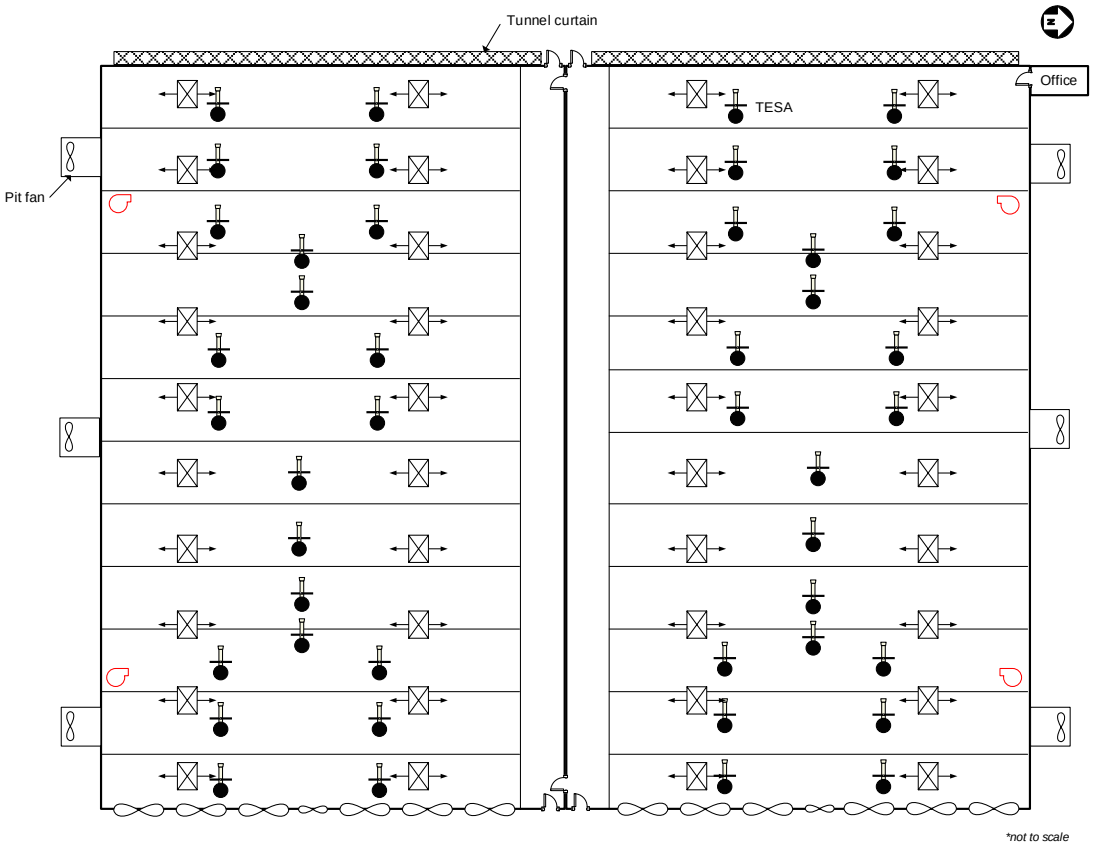

Figure 6. Schematic of TESA installation as a part of a larger study. A total of 44 TESAs were deployed in deep-pit, wean-finish pig facility located within five miles of Pocahontas, IA, USA from August 8th, 2016 to January 25th, 2017.

2.3.1 Data post-processing

Text files were first imported into Matlab (R2017a, The Mathworks, Inc., Natick, Massachusetts, USA) with any rows of data containing un-importable cells excluded (i.e., garbled text, etc.). Each row of data (corresponding to a TESA) was first checked to make sure at least 15 measurements were included in the mean value that was returned by the TESA DAQ. Next, analogue voltages for the thermistors were inspected to be between a rational range of 1 to 4 V_{DC}. Any values outside this range were discarded. Similarly, for the digital T_{db} and RH,

values outside 10 °C to 40 °C and 5% to 100% RH, respectively, were discarded. Data were then saved to .mat files to decrease future processing time. Analogue voltages were then transformed to physical values following the equations given by Gao et al. (2016). Data were filtered again to confirm values were within the measurement limit of the sensors and no erroneous data types were present. All faulty, missing, or discarded data were stored as Not-a-Number.

2.3.2 Mean radiant temperature

For calculation of T_{mr}, the thermal balance (ISO 7726, 2001) equating radiative exchanges of surrounding surfaces to the losses due to convection was solved using the T_g, BGT diameter, assumed emissivity, T_{db}, and airspeed. The standard equation presented in ISO 7726 (2001), assumes the BGT is at steady-state conditions, which is valid when the TE in the room changes slower than the response time of the BGT. In a typical pig production facility, forced air furnaces in the winter cause rapid increases in T_{db}, faster than the response time of the BGT, which consequently falsely decreases the estimation of T_{mr}.

2.4 Field performance evaluation

Once the barn was no longer stocked and prior to washing, the system was powered down and each TESA was enclosed in a yellow plastic bag, and then secured to the ceiling to avoid possible moisture damage from power washing. After the rooms had been cleaned, each TESA was removed from the bag and approximately one week of empty facility data was collected. The Mobile Temperature and Relative Humidity Reference (MTRHR) system was then used to validate the T_{db} and RH sensors of all 44 TESAs.

2.4.1 Experimental setup

The MTRHR featured a 1500 W electric resistance heater with a transition to a 0.1524 m diameter flex duct that contained an inline fan to constantly supply tempered air to a vertical 0.2032 m diameter galvanised round duct (Figure 7). Each TESA was placed inside the vertical duct, near a reference T_{db} and RH sensor (HMP110 with HMT120, Vaisala, Helsinki, Finland). The reference sensor analogue signals were conditioned with a divider circuit and processed with

a 16-bit ADC (ADS-1115, Adafruit Industries LLC, New York City, New York, USA) interfaced with a microcontroller (Arduino Micro, Arduino LLC, Italy).

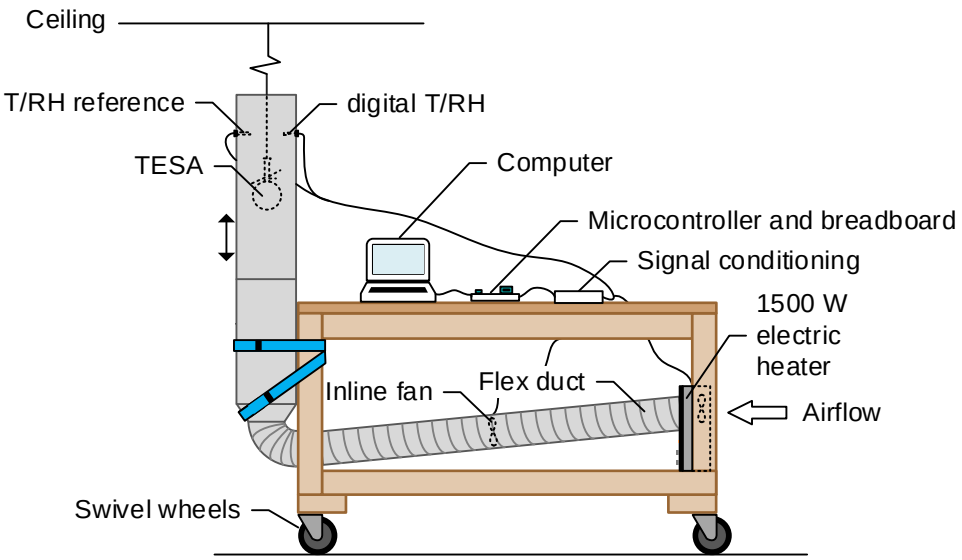

Figure 7. Schematic of Mobile Temperature and Relative Humidity Reference (MTRHR) system used to evaluate each TESA in the facility after about six months of recording.

2.4.2 Procedure

For each sensor, initial conditions and the difference between the initial conditions and the steady-state conditions were uniquely determined due to fluctuating conditions in the room. The initial condition was determined as the mean of 12 measurements (~36 s) prior to the step change. Once in the duct, the sensors were monitored for about 4 to 5 min.

Once the sensor was at steady-state conditions (as determined by the time constant of a first-order model), 12 measurements were randomly selected from the data to decouple the time dependence between measurements. These randomly selected measurements were then averaged to form the mean steady-state value. The same approach was applied to the reference sensor measurements.

2.4.3 Time constant

The time constant of the thermistor T_{db}, digital T_{db}, and RH sensors for each TESA was determined by measuring the response to a step change from the ambient conditions inside the room to the tempered, steady conditions inside MTRHR. A nonlinear, least squares regression (R2017a, The Mathworks, Inc., Natick, Massachusetts, USA) of temperature (equation 1a; step-up) and RH (equation 1b; step-down) versus elapsed time was performed to determine the time constant (τ), assuming first-order system behaviour. The time constant served as a metric to determine the time to reach steady-state conditions, estimated by 4τ (~99% of the steady-state value), to enable subsequent calculation of the mean steady-state value (i.e., single-point calibration value).

$$T_{db}(t) = T_{db_0} + \delta T_{db}\left(1 - e^{\frac{-t+t_0}{\tau}}\right) \quad (1a)$$

$$RH(t) = RH_0 + \delta RH\left(e^{\frac{-t+t_0}{\tau}}\right) \quad (1b)$$

where

$x(t)$	= TESA sensor response as a function of time (°C or %)
x_0	= initial mean sensor value at time t_0 (°C or %)
δx	= difference between x_0 and x at steady-state (°C or %)
t	= time (s)
t_0	= initial time (s)
τ	= time constant (s)

2.4.4 Statistical analysis

A Welch's t-test was performed to determine if the mean reference value was statistically different from the mean TESA sensor value during steady-state conditions with the variances of the sensor and reference assumed to be unequal and estimated from independent assessments of standard uncertainty. Contributors to the zeroth-order uncertainty (Table 2) for the reference T_{db} and RH sensor (provided by the manufacturer) were stated accuracy (±0.2 °C; ±1.5%), factory calibration uncertainty (±1.1%), stability over 2 years (±2%), and analogue output accuracy (HMT120; ±0.1% full scale output signal; ±0.05 °C; ±0.125%).

Table 2. Zeroth-order uncertainty budget for the sources needed to determine the standard uncertainty associated with reference T_{db} and RH measurements.

Parameter	Value	Probability distribution	Divisor	Standard uncertainty
$\Delta^0 T_{ref}$ [a]	0.12 °C	Normal	1	0.12 °C
$\Delta^0 RH_{ref}$ [b]	1% RH	Normal	1	1% RH
ΔR_{ref} [c]	2.49 Ω	Rectangular	√3	1.44 Ω
ΔV_{ref} [d]	3.81 10^{-5} V BL^{-1} [e]	Rectangular	√3	2.20 10^{-5} V BL^{-1}

[a] T_{db} zeroth-order standard uncertainty from manufacturer specifications
[b] RH zeroth-order standard uncertainty from manufacturer specifications
[c] divider resistor (249 Ω) tolerance (±1.0%)
[d] ±0.5 ADS-1115 16-bit ADC resolution = 7.63 10^{-5} V BL^{-1}
[e] Binary Level (BL)

For a single measurement sample, the standard uncertainty associated with the reference T_{db} and RH measurement (equation 2) was determined by propagating the sources (ΔR_{ref} and ΔV_{ref}; Table 2) through the analytical solution derived from the divider circuit (Appendix A).

$$\Delta x_{ref}{}^2 = \left(\frac{\partial x_{ref}}{\partial V_{ref}} \Delta V_{ref}\right)^2 + \left(\frac{\partial x_{ref}}{\partial R_{ref}} \Delta R_{ref}\right)^2 \quad (2)$$

where

Δx_{ref} = single sample reference standard uncertainty (°C or % RH)
ΔV_{ref} = analogue voltage standard uncertainty (V_{DC})
ΔR_{ref} = divider resistor standard uncertainty (Ω)

The combined standard uncertainty associated with the mean steady-state T_{db} and RH reference (equation 3) was determined as the root-sum square of the standard uncertainty associated with each sample (equation 2) comprised in the mean, the zeroth-order standard uncertainty (Table 2), and the standard error of the mean steady-state value.

$$\Delta \bar{x}_{ref}{}^2 = \frac{\sum \Delta x_{ref}{}^2}{n} + \left(\Delta^0 x_{ref}\right)^2 + \left(\frac{s_{ref}}{\sqrt{n}}\right)^2 \quad (3)$$

where

$\Delta \bar{x}_{ref}$ = mean steady-state reference combined standard uncertainty (°C or % RH)
$\Delta^0 x_{ref}$ = zeroth-order standard uncertainty for reference sensor (°C or % RH; Table 2)

s_{ref} = steady-state standard deviation for reference sensor (°C or % RH)
n = number of steady-state measurements

Similarly, for a given TESA sensor, the combined standard uncertainty associated with the mean steady-state value (equation 4) was determined as the root-sum square of the zeroth-order standard uncertainty (Table 1), and the standard error of the mean steady-state value.

$$\Delta\bar{x}_{TESA}{}^2 = (\Delta^0 x_{TESA})^2 + \left(\frac{s_{TESA}}{\sqrt{n}}\right)^2 \quad (4)$$

where
$\Delta\bar{x}_{TESA}$ = mean steady-state TESA combined standard uncertainty (°C or % RH)
$\Delta^0 x_{TESA}$ = zeroth-order standard uncertainty for TESA sensor (°C or % RH; Table 1)
s_{TESA} = steady-state standard deviation for TESA sensor (°C or % RH)

Equation 5 provides the basis for a hypothesis test whether a TESA sensor was unacceptable (i.e., significant bias exists). Assuming $\bar{x}_{TESA}$ and $\bar{x}_{ref}$ are distributed according to a normal distribution with the standard error estimated by equation 3. Then, z-statistic is distributed according to a normal distribution with mean zero and unity variance, with infinite degrees of freedom. The test for significance was two-sided.

$$z_{calc} = \frac{\bar{x}_{TESA} - \bar{x}_{ref}}{\sqrt{\Delta\bar{x}_{TESA}{}^2 + \Delta\bar{x}_{ref}{}^2}} \quad (5)$$

where
z_{calc} = z-statistic
$\bar{x}_{TESA}$ = mean TESA sensor steady-state value (°C or % RH)
$\bar{x}_{ref}$ = mean reference steady-state value (°C or % RH)

For $\bar{x}_{ref}$ found to be significant ($p < 0.05$), a bias correction was applied to the TESA sensor measurement (equation 6).

$$x'^*_{TESA} = x'_{TESA} + \left(\bar{x}_{TESA} - \bar{x}_{ref}\right) \quad (6)$$

where
x'^*_{TESA} = bias corrected future measured value (°C or % RH)
x'_{TESA} = future measured value (°C or % RH)

Since it was infeasible to have a calibration reference wind tunnel present for the OTA, airspeed was assessed on a relative basis, that is, Chauvenet's criterion with a maximum allowable deviation of less than 2.52 was used to eliminate outliers, and a box-and-whisker diagram was utilised to visualise the data.

3 Results and discussion

3.1 Thermal environment sensor array

A TESA was estimated to cost approximately 120 USD (excluding the cost of labour) for custom PCB, sensors, housing, and accompanying hardware. Additionally, three-conductor wire, the RS-485 bus to USB converter, and a computer were needed. The concept of TESA is similar to networks created for commercial buildings to calculate and/or control predicted mean vote (Tse & Chan, 2008; Ye, Yang, Chen, & Li, 2003), except that TESA has been sealed and weatherproofed to be suitable for animal production environments.

3.2 Field deployment

The TESA DAQ system was deployed inside the facility for 170.5 d and on average (95% CI), collected 154.5 d (152.2, 156.9) of data at a sampling interval of approximately 1.1 min. This sampling interval was longer than originally targeted (1 min) due to the increase in wire between TESA DAQs that had not been previously tested. Total number of usable measurements (after post-processing) for all sensors per TESA averaged 202,310 (199,187, 205,437). The minimum and maximum total number of measurements for all TESAs were 164,124 and 207,280, respectively.

The most common cause for data loss during deployment was attributed to automatic updates restarting the operating system of the notebook computer running the CDMS (accounted for ~10 days). Other issues included the CDMS consuming too much memory, which required a restart of the notebook computer. Future CDMS should be developed using a Linux platform and be tested to ensure no memory leaks exist or perform a scheduled system reboot. Other problems

encountered included several sensors malfunctioning for unknown reasons; they were replaced as soon as it was possible. Scrambled data were encountered from several TESA DAQs and this was often attributed to loose wires at the screw terminals and occasionally a failed RS-485 to RS-232 converter.

Both wireless and wired sensor networks (i.e., signal transducers plus DAQ and transmission) have been developed using a variety of communication protocols and hardware interfaces to monitor indoor TE, each with a diverse range of successes and challenges (Ali, Zanzinger, Debose, & Stephens, 2016; Darr & Zhao, 2008; Darr, Zhao, Ehsani, Ward, & Stombaugh, 2005; Tse & Chan, 2008). Wireless sensor networks offer reduced installation labour and time as sensors and nodes can easily be placed throughout a building and lack long connecting wires; however, this can adversely affect costs, and require optimisation of the location of network nodes and base stations to ensure data transmission is reliable. Also, if the terminal nodes are powered by a portable power source (e.g., batteries), labour is required to ensure the network has power.

Dust accumulation on all the sensors, except the OTA, was observed within the first several weeks. The OTA was maintained at approximately 100 °C, which was able to burn the dust particles before they were able to accumulate on the heated thermistor. The digital T_{db} and RH sensor was intentionally mounted with sensing elements pointing down (Figure 1) and the back of the sensor housing facing upwards. This approach lessened the effect of dust; however, the results of the field performance evaluation do show some variability among sensors. The top half of the BGT accumulated a thicker film of dust, which will have had a subsequent effect on the emissivity and response time of the BGT. Dust in livestock and poultry facilities is still a major barrier for implementing advanced measurement systems. An active purge system (puffs of air) to remove/prevent dust accumulation or “self-cleaning” surface coatings may have potential to reduce dust-related problems for livestock facility sensors.

In total, for all 44 TESAs each with five sensors, approximately 40.5 million data were collected. The total quantity of data collected and its spatial discretisation achieved with the

TESA DAQ system will allow future data mining techniques to explore how the controllers and facility itself respond to changing climate conditions.

3.3 Field performance evaluation

Once the time to reach steady-state (4τ) was determined for each thermistor T_{db} and digital T_{db} and RH sensors, for all 44 TESAs, the mean TESA sensor value was statistically compared to the mean reference value during steady-state conditions.

3.3.1 Time constant

The time to reach steady-state and nonlinear regression statistics are summarised in Table 3 for all 44 TESA thermistor T_{db}, digital T_{db}, and digital RH sensors. Examples of the data and first-order regression model fit are shown in Figure 8. While the results of the analysis are unique to each TESA sensor, the summary in Table 3 provides insight to the overall performance of the group of sensors. Since the TE inside the facility during the field performance evaluation was dynamic, x_0 were uniquely determined for each sensor; hence, variation in this mean of this value were anticipated. The difference between x_0 and x at steady-state (i.e., δx) was expected to have low variation as the heat source (1500 W) and inline fan flowrate were constant. Due to small tolerances achieved in today's sensor manufacturing, τ should also have low variation; however, differences in τ between sensors was most likely attributed to the conditions the sensors experienced inside the barn. Time to reach steady-state was greatest for RH and smallest for the T_{db} thermistor (Table 3). The RH sensing mechanism (capacitance) is susceptible to particulate matter accumulation and can easily result in longer response time and inaccurate measurements. The RMSE provides an estimate of the overall uncertainty over the regression and the validity of the first-order behaviour assumption. In addition, inspection of coefficient of determination (R^2) for all sensors showed the nonlinear regression model accounted for greater than 89% of the variance.

Table 3. Summary of average (95% CI) of time to reach steady-state (4τ) and nonlinear regression statistics for the thermistor T_{db}, digital T_{db}, and digital RH sensors for all TESA (n = 44).

Parameter	x_0 (°C or % RH)	δx (°C or % RH)	τ (s^{-1})	4τ (s)	RMSE (°C or % RH)	R^2
T_{db}	13.84 (13.14, 14.53)	6.71 (5.96, 7.46)	21.79 (13.38, 30.21)	87.17 (53.5, 120.84)	0.4 (0.19, 0.61)	0.89 (0.83, 0.96)
$T_{db,d}$	11.87 (11.37, 12.38)	8.69 (8.03, 9.34)	45.84 (33.74, 57.94)	173.8 (124.15, 223.46)	0.33 (0.17, 0.5)	0.96 (0.92, 1)
RH	27.4 (25.08, 29.72)	23.69 (20.95, 26.43)	52.2 (40.76, 63.64)	208.8 (163.04, 254.55)	0.81 (0.48, 1.14)	0.96 (0.92, 1)

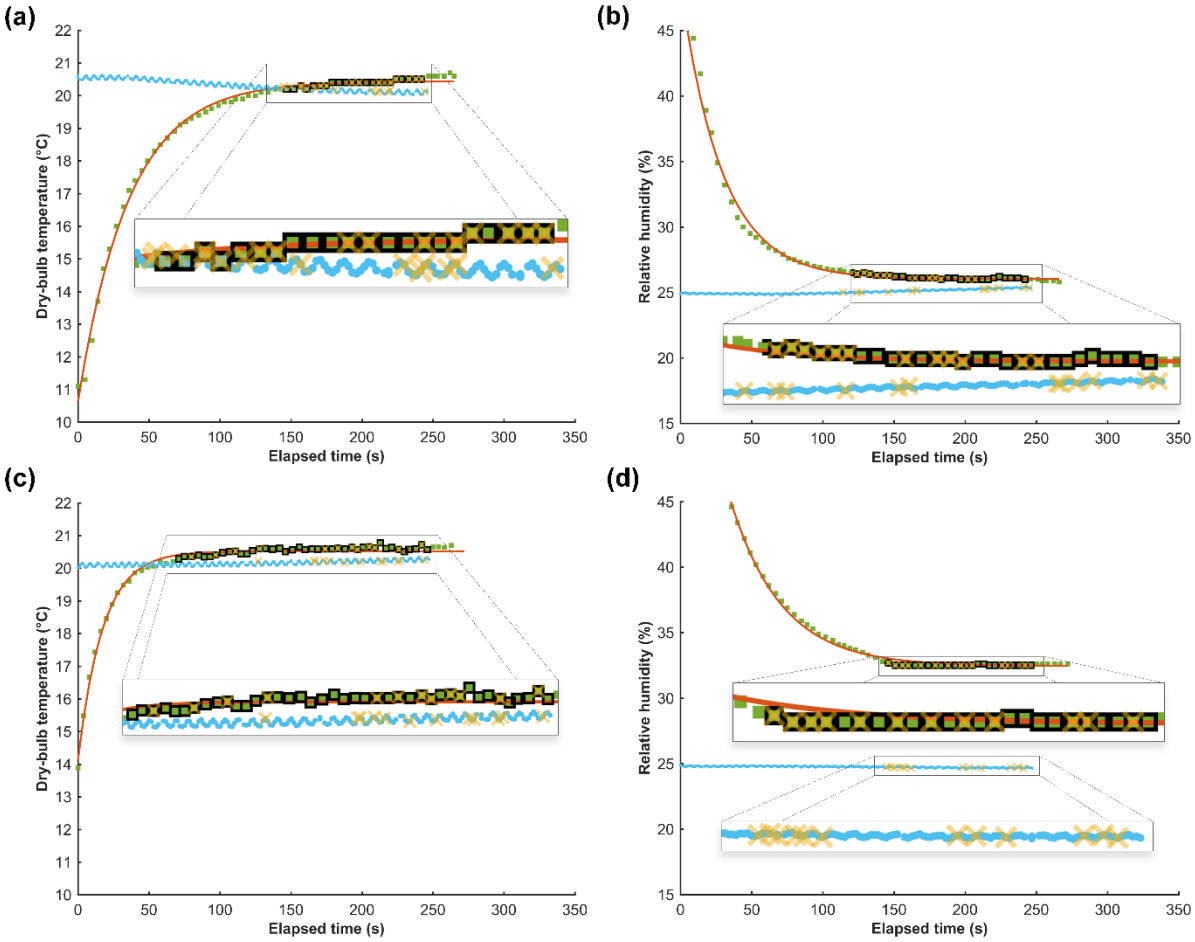

Figure 8. Example of first-order model fit (red line) to TESA T_{db} thermistor (a), RH (b and d), and digital T_{db} (c) data (blue square) and measurements that were randomly selected (denoted X) from the estimated time to reach steady-state (denoted O) for both TESA and the reference. TESA sensors in (a), (b), and (c) did not require a bias correction, while (d) was found to be significantly different from the reference.

The time to reach steady-state was used to determine when steady-state conditions in the MTRHR system were achieved and the sensors could be calibrated. Also, this analysis provides

insight into the response time of the sensors and the subsequent information that can be discerned from the data (i.e., ventilation response and the rate at which the TE changes inside the room).

3.3.2 Calibration

A summary of the input parameters for equation 5 to calculate the z-statistic for assessing whether a significant bias existed between the steady-state TESA and reference sensor values is presented in Table 4. Figure 7 shows examples of data during the steady-state and which data were randomly selected to estimate the mean used for the significance test (equation 6). While the decision to correct measurements of a single TESA sensor was uniquely determined for each sensor, the summary in Table 4 provides insight into the overall performance of the group of sensors. The standard deviation of the steady-state for both TESA and reference sensors was small, as anticipated. In summary, 3 T_{db} thermistor, 4 digital T_{db}, and 12 RH sensors required correction after the 170.5 d inside the facility. Typically, RH sensors do not perform well in dusty and high ammonia environments. Overall, given the cost and accuracy of the selected digital T_{db}/RH sensor in this study, they performed quite well.

Table 4. Summary of parameters for in-field calibration of all TESA thermistor T_{db}, digital T_{db}, and digital RH TESA sensors.

	Range (min, max) [a]						
Parameter	$\bar{x}_{TESA}$ (°C or %RH)	s_{TESA} (°C or %RH)	$\Delta\bar{x}_{TESA}$ (°C or %RH)	$\bar{x}_{ref}$ (°C or %RH)	s_{ref} (°C or %RH)	$\Delta\bar{x}_{ref}$ (°C or % RH)	Failure percent[b]
T_{db}	15.32 - 23.42	0.03 - 4.32	0.31 - 1.29	14.84 - 21.4	0.01 - 18.38	0.37 - 5.33	6.8%
$T_{db,d}$	17.19 - 25.54	0.04 - 3.06	0.31 - 0.94	14.84 - 21.4	0.01 - 18.38	0.37 - 5.33	9.1%
RH	3.79 - 44.15	0.03 - 6.24	1.42 - 1.67	16.78 - 33.55	0.03 - 16.38	1.17 - 4.88	27.3%

[a] n = 44

[b] that is, number of sensors that require bias correction ($p < 0.05$)

The standard uncertainty associated with the mean steady-state TESA and reference sensors was an estimate of the variance from the random sampling error (independent steady-state measurements) and the manufacturer's specifications. For a single measurement, Δx_{ref} was larger than anticipated, and after further inspection by a sensitivity analysis of the input parameters, the divider resistor tolerance (±1%) accounted for more than 98% of the total uncertainty. The other

two sources of uncertainty ($\Delta^0 x_{ref}$ and SE) combined to only account for less than 6% of the total uncertainty associated with $\Delta\bar{x}_{ref}$. Even though the reference sensor was produced with high accuracy (low uncertainty), the required signal conditioning circuit (i.e., divider resistor) to obtain an analogue voltage ultimately increased $\Delta\bar{x}_{ref}$. Signal conditioning circuits should utilise low tolerance (< ±1%) resistors. The lack of necessary signal conditioning circuitry for digital sensors is a major benefit.

Figure 9 graphically depicts the mean OTA airspeeds for each TESA obtained during calibration. Four OTAs were determined to require replacement. While there is some variability in data (~1.5 to ~3.5 m s^{-1}), it is difficult to discern the source. It may be attributed to the physical properties of the OTA changing over time (as a result of being continuously heated or dust) or the experimental method. Turbulence caused by the elbow and flex duct may have affected airspeed results. Further, OTA position (near the centre or near the wall) could explain the large range of values.

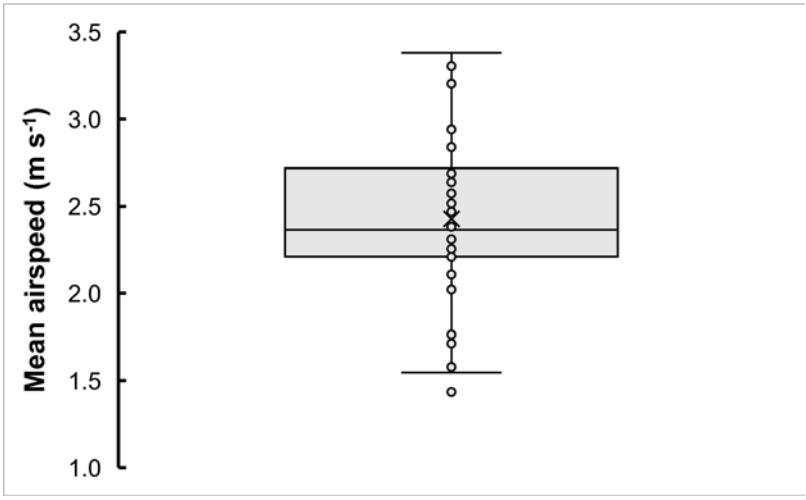

Figure 9. Box-and-whisker diagram for OTA during calibration.

4 Conclusions

A TESA and accompanying DAQ were developed and validated with a well-documented statement of measurement uncertainty for capturing the TE spatial distribution and temporal distribution in pig facilities. The utilisation of low-cost sensors, open-source software, and

microcontroller-based control allowed this novel network to provide sufficient measurement density to promote future studies of the uses of TE data in livestock and poultry facilities.

A TESA can provide a complete description of parameters that influence the rate of heat exchange via the different modes (except conduction) that an animal experiences in its surroundings. Further, a network of TESAs allows for a high level of spatial discretisation such that different regions of a facility can be evaluated in terms of uniformity, ventilation system performance, and ventilation controller performance. The capabilities of a TESA DAQ system support an enhanced ability to create and validate computational models that often lack all the TE parameters and discretisation.

Livestock and poultry facility environments are difficult to instrument and maintaining quality measurements over time is even more challenging. The TESA DAQ system offers a robust approach to instrumenting these environments, while accepting that sensors must be periodically cleaned and verified in order to maintain high sensor performance. Further, a modified t-test accounting for random error (from sampling) and sensor performance (manufacturer specifications) was created for conducting the single-point calibration and to determine whether statistically significant bias existed. While T_{db} affects convective and evaporative heat loss, it must be combined with other TE measurements to create a complete description of how an animal exchanges heat with its surrounding. The development of TESA is a necessary advance in precision livestock farming.

4.1 Acknowledgements

This research was supported with funding provided by the Iowa Pork Producers Association under NPB Project 14-242. The authors would like to acknowledge the contributions of undergraduate students Grant Hoppes, Heather Tenboer, and Oluwadurotimi Koya during the preparation and completion of this work.

The research work of Yun Gao was partly supported by the National Key Research and Development Program of China (2016YFD0500506).

5 References

Ali, A. S., Zanzinger, Z., Debose, D., & Stephens, B. (2016). Open Source Building Science Sensors (OSBSS): A low-cost Arduino-based platform for long-term indoor environmental data collection. *Building and Environment*, *100*, 114–126. https://doi.org/10.1016/j.buildenv.2016.02.010

ASHRAE. (2013). *Handbook of fundamentals*. Atlanta, GA: America Society of Heating, Refrigeration and Air Conditioning Engineers.

Beckett, F. E. (1965). Effective Temperature for Evaluating or Designing Hog Environments. *Transactions of the ASAE*, *8*(2), 0163–0166. https://doi.org/10.13031/2013.40457

Bond, T. E., & Kelly, C. F. (1955). The globe thermometer in agricultural research. *Agricultural Engineering*, *36*(4), 251–255.

Bond, T. E., Kelly, C. F., & Heitman Jr, H. (1952). Heat and moisture loss from swine. *Agric. Eng*, *33*(3), 1948–154.

Brown-Brandl, T., Hayes, M., Xin, H., Nienaber, J., Li, H., Eigenberg, R. A., … Shepard, T. (2014). Heat and Moisture Production of Modern Swine. *ASHRAE Transactions*, *120*.

Curtis, S. E. (1983). *Environmental Management in Animal Agriculture*. Ames, IA: The Iowa State University Press.

Darr, M. J., & Zhao, L. (2008). A wireless data acquisition system for monitoring temperature variations in swine barns. American Society of Agricultural and Biological Engineers. https://doi.org/10.13031/2013.25614

Darr, M. J., Zhao, L., Ehsani, M. R., Ward, J. K., & Stombaugh, T. S. (2005). Evaluation of controller area network data collection system in confined animal feeding operations. American Society of Agricultural and Biological Engineers. https://doi.org/10.13031/2013.18363

DeShazer, J. A., Hahn, L., & Xin, H. (2009). Chapter 1: Basic Principles of the Thermal Environment and Livestock Engergetics. In James A. DeShazer, *Livestock Energetics and Thermal Environment Management* (1st ed., pp. 1–22). St. Joseph, MI: American Society of Agricultural and Biological Engineers.

Fournel, S., Rousseau, A. N., & Laberge, B. (2017). Rethinking environment control strategy of confined animal housing systems through precision livestock farming. *Biosystems Engineering*, *155*, 96–123. https://doi.org/10.1016/j.biosystemseng.2016.12.005

Gao, Y., Ramirez, B. C., & Hoff, S. J. (2016). Omnidirectional thermal anemometer for low airspeed and multi-point measurement applications. *Computers and Electronics in Agriculture*.

Hayes, M. D., Xin, H., Li, H., Shepherd, T. A., Zhao, Y., & Stinn, J. P. (2013). Heat and moisture production of Hy-Line brown hens in aviary houses in the Midwestern US. *Transactions of the ASABE*, *56*(2), 753–761.

ISO 7726. (2001). *Ergonomics of the thermal environment — instruments for measuring physical*

quantities. Geneva: International Standardization Organization.

Mount, L. E. (1964). Radiant and convective heat loss from the new-born pig. *The Journal of Physiology*, *173*(1), 96–113.

Mount, L. E. (1967). The heat loss from new-born pigs to the floor. *Research in Veterinary Science*, *8*(2), 175–186.

Pereira, N., Bond, T. E., & Morrison, S. R. (1967). Ping-pong ball into black-globe thermometer. *Agricultural Engineering*, *48*(6), 341.

Purswell, J. L., & Davis, J. D. (2008). Construction of a low cost black globe thermometer. *Applied Engineering in Agriculture. ASABE*, *24*(3), 379–381.

Renaudeau, D., Gourdine, J.-L., & St-Pierre, N. R. (2011). A meta-analysis of the effects of high ambient temperature on growth performance of growing-finishing pigs. *Journal of Animal Science*, *89*(7), 2220–2230.

Tse, W. L., & Chan, W. L. (2008). A distributed sensor network for measurement of human thermal comfort feelings. *Sensors and Actuators A: Physical*, *144*(2), 394–402. https://doi.org/10.1016/j.sna.2008.02.004

UN. (2015). *World Population Prospects: The 2015 Revision, Key Findings and Advance Tables* (No. Working Paper No. ESA/P/WP.241). New York City, NY: United Nations, Department of Economic and Social Affairs, Population Division.

Vilela, M. O., Oliveira, J. L., Teles Junior, C. G., Tinôco, I. F., Baptista, F. J., Barbari, M., … Souza, C. F. (2015). Spatial variation of enthalpy in a commercial broiler house in a hot climate region. Retrieved from https://dspace.uevora.pt/rdpc/handle/10174/17506

Ye, G., Yang, C., Chen, Y., & Li, Y. (2003). A new approach for measuring predicted mean vote (PMV) and standard effective temperature (SET∗). *Building and Environment*, *38*(1), 33–44. https://doi.org/10.1016/S0360-1323(02)00027-6

6 Appendix A

The following equations are the transfer functions for converting reference T_{db} and RH from analogue voltage to a physical value for a single measurement sample. The standard uncertainty of the inputs to equations A.1 and A.2 (ΔR_{ref} and ΔV_{ref}) are propagated through equations A.1 and A.2 to determine the standard uncertainty associated with reference T_{db} and RH measurements (equation 2).

$$T_{ref} = -40\,°\text{C} + (V_{T\_ref} - V_{out,low}) \times \left(\frac{(60\,°\text{C} - (-40\,°\text{C}))}{(V_{out,high} - V_{out,low})} \right) \quad \text{(A.1)}$$

$$RH_{ref} = 0\% + (V_{rh\_ref} - V_{out,low}) \times \left(\frac{(100\% - 0\%)}{(V_{out,high} - V_{out,low})} \right) \quad \text{(A.2)}$$

where

T_{ref} = reference dry-bulb temperature (°C)
V_{T_ref} = measured reference analogue voltage (V_{DC})
$V_{out,low}$ = reference sensor minimum output voltage (V_{DC}; = 4 mA × R)
$V_{out,up}$ = reference sensor maximum output voltage (V_{DC}; = 20 mA × R)
RH_{ref} = reference relative humidity (%)
V_{rh_ref} = measured reference analogue voltage (V_{DC})